

Variations in upper water structure during MIS 3 from the western South China Sea

DU JiangHui & HUANG BaoQi*

MOE Key Laboratory of Orogenic Belts and Crustal Evolution, School of Earth and Space Sciences, Peking University, Beijing 100871, China

Received March 2, 2009; accepted April 29, 2009; published online August 7, 2009

Core 17954 is located in the modern summer upwelling area in western South China Sea, its sediments recorded the variations of upwelling generated by East Asia Summer Monsoon (EASM) during MIS 3. Based on the strict age model of AMS ^{14}C dating, the paleo-Sea Surface Temperature (SST) and Salinity (SSS) are reconstructed by pairing Mg/Ca-Paleothermometer and $\delta^{18}\text{O}$ of planktonic foraminifera *Globigerinoides ruber* (white s.s.). Results show that in Core 17954, the $\delta^{18}\text{O}$ record of *Gruber* has significant millennium fluctuations as the $\delta^{18}\text{O}$ records from NGRIP icecore and Hulu Cave stalagmites, this indicates that the climate changes of western SCS contains both signals from High Latitude of Northern Hemisphere as well as EASM. In order to get more information on upwelling changes, previous records of thermocline and foraminiferal primary productivity in Core 17954 are collected, restudied and compared. Five distinct shallowing periods of thermocline (referred to as S1–S5) are identified in this study. In S1–S4, SST is lower and productivity is higher, these indicate to an enhanced upwelling and strengthened EASM during these periods. And the lower SSS, caused by increasing precipitation or fresh water input, also prove this standpoint.

Mg/Ca, MIS 3, East Asia Summer Monsoon, upwelling, Paleoceanography

Citation: Du J H, Huang B Q. Variations in upper water structure during MIS 3 from the western South China Sea. Chinese Sci Bull, 2010, 55: 301–307, doi: 10.1007/s11434-009-0388-8

Global climate changes of last glacial are characterized by millennium-scale fluctuations in oxygen isotope records. Dansgaard-Oeschger cycle (D-O cycle), which is characterized by alternation of interstadial (IS) and stadial in Greenland ice core [1], and Herinck event (H event), which is an event of sudden iceberg discharge into the North Atlantic [2–4], are identified to be the major components in the fluctuations. In later researches, such variations are widely discovered in different kinds of paleoclimate records besides Greenland icecores and North Atlantic Ocean deep sea sediments, such as Mediterranean vegetation and Austrian Alps stalagmites from Europe; Loess, Hulu cave stalagmites and marine sediments in northern SCS from East Asia, and Cariaco Basin sediments from South America [5–11]. The wide distribution of D-O cycles and H events indicates that rapid climate changes are teleconnectional. Marine Isotope Stage 3 (MIS 3) is a relatively warm period in the last gla-

cial, the millennium-scale fluctuations also characterize it immensely. Investigation of rapid climate changes during MIS 3 should be carried out since it would greatly improve our understanding of sub-orbital scale climate changes.

Evolution of the East Asian monsoon (EAM) during MIS 3 has been copiously reported. Guliya ice core records show that the Qinghai-Tibet Plateau had a 40% increase of precipitation caused by the enhanced EASM at the end of MIS 3 [12]. Results from the planktonic foraminiferal analysis in ODP Site1144 show that warm species decreased but productivity of surface sea water increased simultaneously during 35–29 ka BP and that the winter monsoon would have strengthened in the interval. Besides, the increasing input of Pearl River represents an intense summer monsoon precipitation during 52–46 ka BP [13]. Furthermore, fluctuations in percentage of montane conifers and *Artemisia* pollen indicate to abrupt vegetation and climate changes of Core 17940 in the northern SCS during MIS 3 [14]. So, based on these previous studies, the exploration of the pa-

*Corresponding author (email: bqhuang@pku.edu.cn)

leoceanographic changes in the modern upwelling area of SCS [15] and the correlation between the upwelling and EASM are quite important.

The calculations of temperature and salinity are key tools in Paleoclimatology research. In the last decades, temperature calculations based on the oxygen isotope paleothermometer ($\delta^{18}\text{O}$) [16] and foraminiferal transfer function [17] have both revealed their inevitable limitations. The alkenone (U_k^{37}) thermometer has also been found to be very sensitive to high temperature and can cause errors in tropical areas [18]. The most reliable temperature calculation is Mg/Ca-paleothermometer, which was first discovered in planktonic foraminiferal culture experiment carried out by Nürnberg [19]. And in order to remove the partly dissolution effect of foraminiferal shell, recent studies have focused on the calibration of Mg/Ca-paleothermometer by using sediment trap, core-tops and other methods [20–24]. Present studies also show that residue sea water oxygen isotope ($\delta^{18}\text{O}_{\text{residue}}$) is a good proxy of paleo-Sea Surface Salinity (SSS), which can be recovered from paleo-sea water oxygen isotope ($\delta^{18}\text{O}_{\text{sw}}$) by pairing Mg/Ca derived Sea Surface Temperature (SST) with oxygen isotope paleothermometer [9,25–27]. In this study, we will use Mg/Ca-paleothermometer and $\delta^{18}\text{O}$ of planktonic foraminifera *Globigerinoides ruber* (white s.s) to reconstruct the SST and SSS of the modern upwelling area in western SCS, and then study the changes of upwelling and related EASM during MIS 3 in comparison with the thermocline and foraminiferal productivity records.

1 Materials and methods

Core 17954 (14°47.8'N, 111°31.5'E) was retrieved from the modern summer upwelling region during the Chinese-German cooperation SONNON95 cruise to SCS in 1994 (Figure 1). It was recovered at 1515 m water depth and contained three gravity cores, in which Core17954-2 is used in this study. It had a relatively homogeneous lithology of gray-green silty mud from continental slope sediments and recorded the sedimentary history over the past 200 ka without significant turbid deposition [28]. Core 17954 was subsampled at 1.5 cm intervals for 100–398.5 cm (including MIS 3), 217 samples were collected for microfossils paleontology identification and Mg/Ca ratio measurement. AMS ^{14}C dates and oxygen isotope data of *G. ruber* refer to Yang et al. [28].

The radiocarbon dates younger than 21880 a BP are calibrated using MARINE04 [29], a standard ocean reservoir correction of 400 years and $\Delta R = 11 \pm 40$ a in SCS are applied by the algorithm of the calibration program [29], for older ages we use Fairbanks0107 calibration [30] and the applied ocean reservoir correction is 256 a in SCS [31]. Radiocarbon dates before and after calibrations are shown in Table 1 and Figure 2.

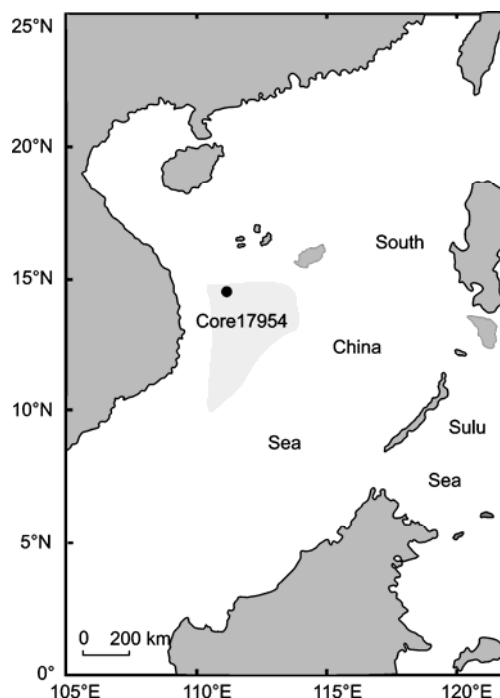


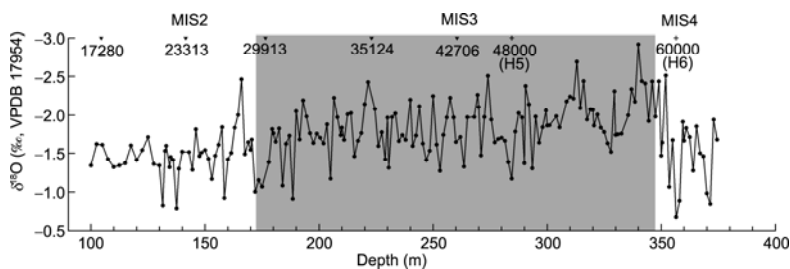
Figure 1 Location of Core 17954 (Modern summer upwelling regions off eastern Vietnam are shaded [15]).

About 30 tests of *Gruber* (size fraction ranges from 0.25 mm to 0.35 mm) are picked for Mg/Ca ratio measurement by ICP-AES in the State Key Laboratory of Marine Geology of Tongji University. The relative standard deviation of Mg/Ca ratio is less than 0.3%. In order to supply a reliable Mg/Ca-paleothermometer estimation, three calibration equations are collated: core-tops calibration in Pacific Ocean from Dekens et al. [21], shell weight calibration from Rosenthal and Lohmann [22] and sediment trap calibration in SCS from Huang et al. [24]. Calibrated result of Dekens and Huang is almost entirely consistent with each other, although the output of Rosenthal and Lohmann shows a considerable offset during the Last Glacial Maximum (LGM), it still reveals a strong agreement during MIS 3. So we chose the calibration of Dekens to estimate our Mg/Ca-SST: $\text{Mg/Ca} = 0.38 \exp [0.09(\text{SST} - 0.61d - 1.6^\circ\text{C})]$, where the Mg/Ca is in mmol/mol and SST is in $^\circ\text{C}$. d is water depths (in km) The standard deviation of this equation is 1.2 $^\circ\text{C}$ [21].

For the purpose of getting a more accurate paleosalinity record, we use the *Gruber* (white) paleotemperature equation of Mulitza et al. [32] to estimate the $\delta^{18}\text{O}_{\text{sw}}$: $\delta^{18}\text{O}_{\text{sw}} = (\text{SST} - 14.2)/4.44 + \delta^{18}\text{O}$, and convert PDB standard to SMOW standard by adding 0.27‰. Afterwards, a high-resolution sea level changes record from Arz et al. [33] and the $\delta^{18}\text{O}_{\text{sw}}$ variations caused by global sea level changes from Waelbroeck et al. (0.00846‰/m sea level) [34] are applied to removing the contribution of sea level changes to $\delta^{18}\text{O}_{\text{sw}}$, and then gets the $\delta^{18}\text{O}_{\text{residue}}$ as a relative robust proxy of SSS [9, 27].

Table 1 Calibration of AMS ^{14}C dates from Core 17954

	Lab ID	Depth (cm)	Species	AMS ^{14}C age (a BP)	Calibrated age (cal a BP)	Error (a)	Method
1	BA05861	104.5	<i>G. ruber</i>	14810±50	17280	227	Marine04 [29]
2	BA05862	141.5	<i>G. ruber</i>	19950±60	23313	234	Marine04 [29]
3	BA05863	176.5	<i>G. ruber</i>	25180±80	29913	189	Fairbanks0107 [30]
4	BA05864	223	<i>G. ruber</i>	29960±120	35124	176	Fairbanks0107 [30]
5	BA05865	260.5	<i>G. ruber</i>	37920±180	42706	234	Fairbanks0107 [30]
6	BA05935	302.5	<i>G. ruber</i>	39800±200	44325	256	Fairbanks0107 [30]

**Figure 2** Western SCS $\delta^{18}\text{O}$ record of *Gruber* versus depth in Core 17954. Triangles denote depths of AMS radiocarbon dates and crosses denote location of two age control points identified from Heinrich events (H5 and H6).

2 Results and discussion

2.1 Age model and $\delta^{18}\text{O}$ record of Core 17954

In order to get a longer and dependable age model, we compare $\delta^{18}\text{O}$ curve of *Gruber* from Core 17954 with the $\delta^{18}\text{O}$ curves from NGRIP icecore (North Greenland Icecore Project members, 2004) [35] and Hulu Cave stalagmites [8]. By comparing, we discard the unreliable ^{14}C age at 302.5 cm. In addition, H5 and H6 events in Core 17954 are identified and are used as another two event age control points. Defined at 284.5 cm, H5 event corresponds to H5' of Hulu Cave and H5 of NGRIP with the age of 48 ka. Meanwhile, H6 event, defined at 356.5 cm, corresponds to H6 from Hulu Cave and NGRIP both with the age of 60 ka [8,35] (Figure 2).

Based on calibrated ^{14}C dates and event age control points, linear interpolation is used to construct the age model of Core 17954 (Figure 3). The average sedimentation rate is 5.9 cm/ka. Samples used for this study ranged between 17 ka and 68 ka (but in our discussion, we just focus on the interval from 20 ka BP to 65 ka BP, including MIS 3).

Millennium-scale rapid fluctuations also characterize $\delta^{18}\text{O}$ record of Core 17954. Identification and age determination of the major H events and D-O cycles in Core 17954 are accomplished by comparison (Figure 3). Overall, $\delta^{18}\text{O}$ curve of Core 17954 is much more similar to the curve from Hulu Cave than NGRIP. While recent researches have shown that the mechanism of millennium-scale variations has a key relationship to monsoon system in low latitude [11], the similarity of climate record between Core 17954 and

Hulu Cave may reveal the analogous mechanism, because the $\delta^{18}\text{O}$ of Hulu Cave stalagmites is a direct indicator for the precipitation brought by EAM [8]. Moreover, in previous studies, discovery of orbital frequencies of 41 ka and 23 ka in $\delta^{18}\text{O}$ record of Core 17954 [36] demonstrates the influence of high-latitude Northern Hemisphere climate on western SCS. So, the climate changes in the western SCS are significantly impacted by both low and high latitude signals

2.2 Mg/Ca-SST and the $\delta^{18}\text{O}_{\text{residue}}$ changes

Mg/Ca derived SST in Core 17954 ranges from 23.1°C to 26.7°C, and averages about 25.0°C (Figure 4(b)). Before 50 ka BP, larger amplitude in SST is revealed. During the LGM (~21.4 ka), the SST is 23.0°C, about 4.5°C lower than modern annual average temperature of 27.5°C¹⁾. Similarly, 4–5°C cooling during LGM is also obtained in site 1145 [9]. However, in H events, decrease of SST in Core 17954 is less than 2°C, that is much smaller than in other sea areas [11]. $\delta^{18}\text{O}_{\text{residue}}$ changed from -0.77‰ to 0.94‰, and averages about 0.2‰ during MIS 3 (Figure 4(c)). In both curves of $\delta^{18}\text{O}_{\text{residue}}$ and SST, obvious millennium-scale fluctuations are unveiled (Figure 4(b), (c)), in which the appearance of relative lower (higher) SSS/ $\delta^{18}\text{O}_{\text{residue}}$ and SST has a strong correspondence to interstadials (stadials) (Figure 4).

2.3 Upwelling and EASM changes indicated by multiple proxies

To investigate the changes of upwelling and EASM in western SCS, foraminiferal transfer functions had already been used to reconstruct the SST, thermocline depth, foraminiferal productivity and other proxies of upwelling in the for

1) National Oceanographic Data Center. World Ocean Atlas 2005. <http://www.nodc.noaa.gov/OC5/WOA05F/woa05f.html>

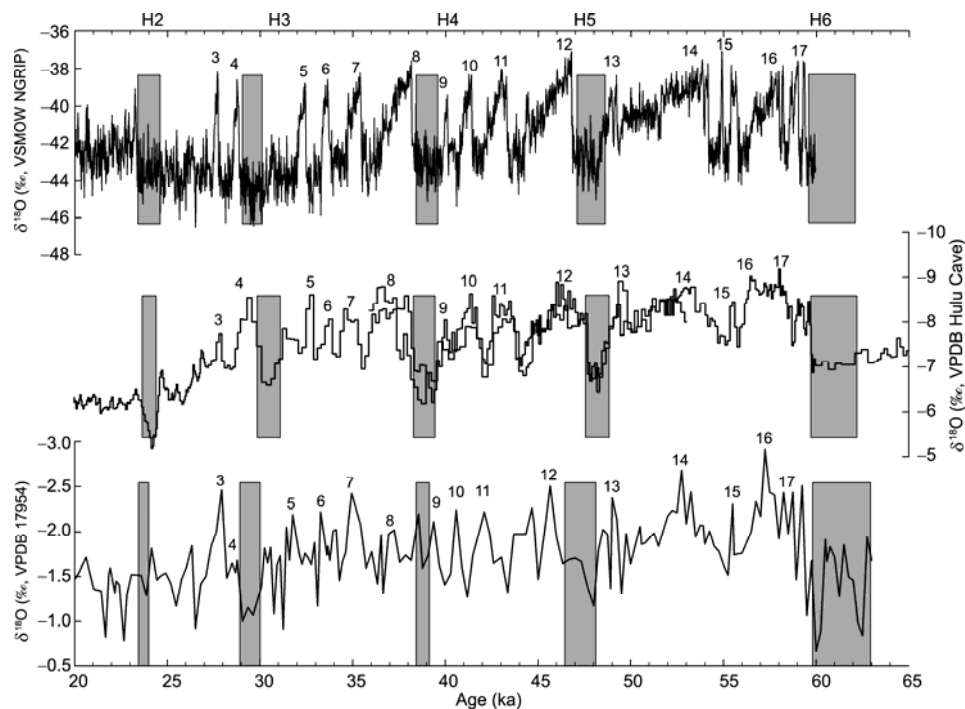


Figure 3 Oxygen isotope stratigraphy of Core 17954 with the comparison of oxygen isotope records from Greenland (NGRIP) and Hulu Cave between 20–65 ka [8,35]. IS events and H events are indicated (H events in all curves are denoted by rectangles and filled with light grey).

mer studies, results show that EASM was strong during interglacials and declined gradually since MIS5 [28,36–38].

In this study, these upwelling proxies are indispensable for understanding the appearance of relative lower (higher) SSS/ $\delta^{18}\text{O}_{\text{residue}}$ and SST during interstadials (stadials). Occurrence of lower (higher) SSS during interstadials (stadials) was also found in ODP Site 1145 and Site 1144 in northern SCS, as well as Sulu Sea and the western Pacific warm pool [9,39–41], it was thought to be caused by the increasing (decreasing) of precipitation brought by super El Niño–Southern Oscillation (ENSO) and to connect to EAM [41]. In these areas, the most important influence of SSS is precipitate–evaporate processing controlled by ESM directly. So, in the similar oceanographic situations, SSS changes of Core 17954 should have the same mechanism that is the appearance of lower SSS during interstails (stadials) was caused by increasing precipitation or fresh water input linked to EASM.

However, SST record of Core 17954 shows quite an opposite way of changing compared to other areas in SCS. This contradiction strongly indicates to the significant influence of upwelling on Core 17954 because these areas are in one sea basin and no other consequential factors can cause such contradiction.

Designed to get further information, we restudy the data of thermocline and foraminiferal primary productivity from Yang et al. [28] by adapting the records to our age model. We find there are five distinct shallowing periods of thermocline in Core 17954, which are 25.5–26.8 ka BP, 30.8–32.3 ka BP, 36.3–39.3 ka BP, 48–50.6 ka BP and 55.7–57 ka BP, and are referred to as S1–S5 orderly (Figure

4(d)). Productivity derived from percentage content of high productivity planktonic foraminiferal species *Neoglobobulimina dutertrei* and *Globigerina bulloides* has a mutual agreement to thermocline result (Figure 4(d), (e)). Like SST and SSS, millennium-scale variations can be easily seen in thermocline and productivity results too. By comparing to $\delta^{18}\text{O}$ curve, S1–S4 can orderly correlate to the interstadial after IS3, IS5, IS8 and IS13, and only S5 correlates to the stadial between IS15 and IS16. In these interstadials, productivity is also relative high. So, we argue that in S1–S4, which are synchronous with interstadials, the presences of shallower thermocline, lower SST and higher productivity, is caused by enhanced upwelling. And the coexisted lower SSS is generated by increasing precipitation or fresh water input. Both these two explanations demonstrate that EASM was intense during S1–S4. This interpretation also coincides with the result from Hulu Cave which indicates to an enhancement of EASM during interstadials [8]. However, we cannot know whether the upwelling was increased or not during S5, for it is synchronous with the stadial and the cold climate condition can also bring the same paleoceanographic changes. At last, unfortunately limited by the time resolution of our materials, discussions of paleoceanographic proxies and their relationship to EASM are confined to S1–S4 which have obvious shallowing thermocline to identify. As to the appearances of lower (higher) SST and SSS in other interstadials (stadials), whether they have a close relationship to strengthened (weakened) EASM or not cannot be clearly seen; further study with higher resolution materials will resolve this problem.

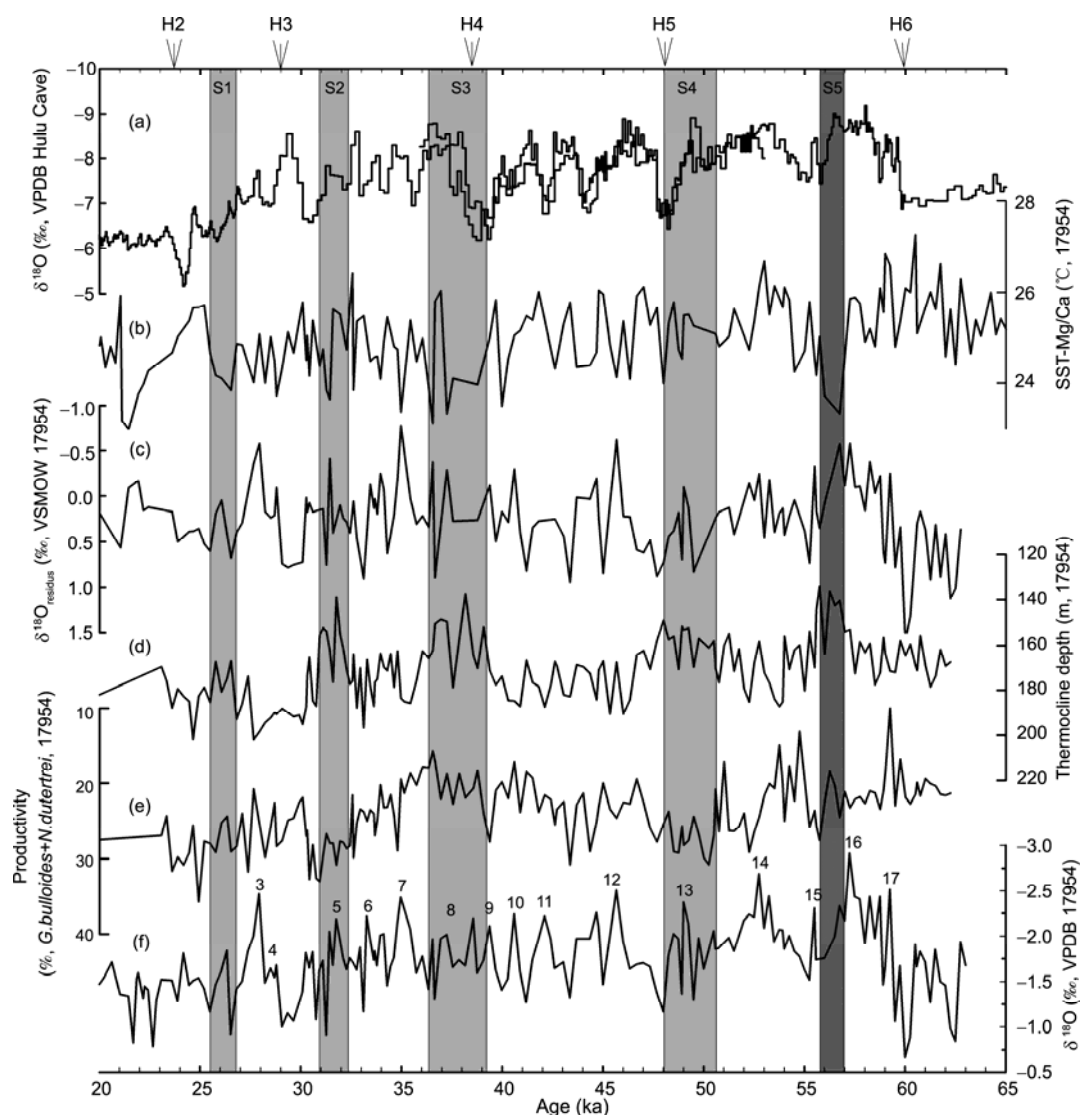


Figure 4 Multiple proxies indicated paleoceanographic changes of upper ocean structure from Core 17954 with comparison to $\delta^{18}\text{O}$ record from Hulu Cave. (a) $\delta^{18}\text{O}$ record from Hulu Cave [8]. (b) Mg/Ca-SST record from Core 17954. (c) $\delta^{18}\text{O}_{\text{residue}}$ (proxy of SSS) record from Core 17954. (d) Thermocline depth derived from foraminiferal transfer function from Core 17954 [28]. (e) Productivity derived from percentage content of high productivity planktonic foraminiferal species *Neogloboquadrina dutertrei* and *Globigerina bulloides* from Core 17954 [28]. (f) $\delta^{18}\text{O}$ record of *G. ruber* from Core 17954. Rectangle areas indicate to the period of shallowing thermocline (S1–S5). Light grey is filled in S1–S4 and dark grey is filled in S5.

Meanwhile, our results hint that to use SSS as a regional proxy of upwelling is inappropriate. SSS in low-latitude sea areas are controlled by atmosphere-ocean heat and vapour transitions directly; the influence of upwelling seems to be inconsequential. At present, many studies attempt to use $\delta^{18}\text{O}_{\text{residue}}$ as a proxy of salinity to represent evaporation-precipitation changes, and particularly focus on the study of the strong influence on hydrological cycles and precipitation brought by Intertropical Convergence Zone (ITCZ) [11,42, 43]. Study of the sedimentary records from Cariaco Basin showed that when the H events occurred, the southward shift of ITCZ in the Central America region could cause quite contrary changes of salinity on different side of Panama Strait: in Eastern Tropical Pacific, seawater would be saltier but in Caribbean Sea it would be fresher. Thus the North At-

lantic Deep Water (NADW) could not be formed because the Gulf Stream whose water source is from Caribbean Sea was fresher than usual. Then the Great Ocean Conveyor broke off and millennium-scale abrupt climate changes happened [11]. The standpoint of which the thermohaline variations can cause rapid climate changes is widely supported [44]. The modeling of Schiller et al. confirmed that the increase of radial temperature gradient in North Hemisphere would cause southward migration of ITCZ in Atlantic Ocean [45]. Paleoceanographic records from Core 17954 may note the same point: during H events, SST decreased quite less than Eastern Tropical Pacific Ocean, so the increase of radial temperature gradient in North Hemisphere might really exist during H events. But whether such changes link to long-term ENSO [41,46] or not still needs further research.

3 Conclusions

Based on the estimation of SST and $\delta^{18}\text{O}_{\text{residue}}$ (the proxy of SSS), investigation of the paleoceanographic changes of upper water in western SCS and their relation to EASM are conducted.

(1) The $\delta^{18}\text{O}$ record of *G. ruber* is characterized by millennium-scale variations in Core 17954. Heinrich events (H2–H6) and D-O cycles (IS3–17) are identified by comparing to the $\delta^{18}\text{O}$ curves from Greenland NGRIP icecore and Hulu Cave stalagmites. The climate changes in the western SCS contain both northern high latitude signal and tropical-low latitude signal, but the latter may be more important since they are connected by EASM and the precipitation it brought.

(2) SST and SSS records of Core 17954 both reveal distinct millennium-scale variations; in the interstadials (stadials) SSS and SSS both are lower (higher).

(3) The thermocline record of Core 17954 has five obvious shallowing periods (S1–S5), in which S1–S4 coincide with the interstadials and are accompanied by lower SST and higher productivity. This demonstrates that the upwelling was strengthened in these intervals, while the lower SSS indicates that the precipitation increased additionally; both suggest that the EASM was relatively intense in these periods.

We thank the Earth Science Department of Kiel University for providing samples, State Key Laboratory of Marine Geology of Tongji University for carrying out planktonic foraminiferal Mg/Ca analysis. The special thanks should be delivered to Dr. Xu Jian who reviewed our manuscript and gave valuable suggestions. This work was supported by the National Basic Research Program of China (Grant No. 2007CB 815901), National Natural Science Foundation of China (Grant No. 40306007) and State Key Laboratory of Paleobiology and Stratigraphy (Grant No. 033109).

- 1 Dansgaard W, Johnsen S J, Clausen H B, et al. Evidence for general instability of past climate from a 250-kyr ice-core record. *Nature*, 1993, 364: 218–220
- 2 Heinrich H. Origin and consequences of cyclic ice rafting in the northeast Atlantic Ocean during the past 130,000 years. *Quat Res*, 1988, 29: 142–152
- 3 Bond G, Heinrich H, Broecker W S, et al. Evidence for massive discharges of icebergs into the North Atlantic Ocean during the last glacial period. *Nature*, 1992, 360: 245–249
- 4 Broecker W S. Massive iceberg discharges as triggers for global climate change. *Nature*, 1994, 372: 421–424
- 5 Tzedakis P C, Frogley M R, Lawson I T, et al. Ecological thresholds and patterns of millennial-scale climate variability: the response of vegetation in Greece during the last glacial period. *Geology*, 2004, 32: 109–112
- 6 Spötl C, Mangini A. Stalagmite from the Austrian Alps reveals Dansgaard-Oeschger events during isotope stage 3: Implications for the absolute chronology of Greenland ice cores. *Earth Planet Sci Lett*, 2002, 203: 507–518
- 7 Fang X M, Ono Y, Fukusawa H, et al. Asian summer monsoon instability during the past 60,000 years: Magnetic susceptibility and pedogenic evidence from the western Chinese Loess Plateau. *Earth Planet Sci Lett*, 1999, 168: 219–232
- 8 Wang Y J, Cheng H, Edwards R L, et al. A high-resolution absolute-dated late Pleistocene monsoon record from Hulu Cave, China. *Science*, 2001, 294: 2345–2348
- 9 Oppo D W, Sun Y. Amplitude and timing of sea-surface temperature change in the northern South China Sea: Dynamic link to the East Asian monsoon. *Geology*, 2005, 33: 785–788
- 10 Peterson L C, Haug G H, Hughen K A, et al. Rapid changes in the hydrological cycle of the tropical Atlantic during the last glacial. *Science*, 2000, 290: 1947–1951
- 11 Leduc G, Vidal L, Tachikawa K, et al. Moisture transport across Central America as a positive feedback on abrupt climatic changes. *Nature*, 2007, 445: 908–911
- 12 Shi Y F, Yu G, Liu X D, et al. Reconstruction of the 30–40 ka BP enhanced Indian monsoon climate based on geological records from the Tibetan Plateau. *Palaeogeogr Palaeoclimatol Palaeoecol*, 2001, 169: 69–83
- 13 Huang B Q, Yang W Y. Variations of upper water structure in MIS 3 from the northern South China Sea (in Chinese). *Quat Sci*, 2006, 26: 436–441
- 14 Luo Y L, Sun X J. Millennial-scale climatic fluctuations in pollen record of deep deposit from South China Sea (in Chinese). *Quat Sci*, 1999, 6: 536–540
- 15 Wiesner M G, Zheng L, Wong H K, et al. Fluxes of particulate matter in the South China Sea. In: Ittekkot V, Schöfer P, et al., eds. *Particle Fluxes in the Ocean*. London: John Wiley & Sons Ltd, 1996. 293–312
- 16 Emiliani C. Pleistocene temperatures. *J Geol*, 1955, 63: 538–578
- 17 Imbrie J, Kipp N G. A new micropaleontological method quantitative paleoclimatology: application to a late Pleistocene Caribbean core. In: Turekian K K, ed. *The Late Cenozoic Ice Ages*. New Haven and London: Yale University Press, 1971. 71–181
- 18 Herbert T D. Alkenone Paleotemperature Determinations. In: Elderfield H, ed. *The Oceans and Marine Geochemistry*. Vol. 6, In: Holland H D, Turekian K K, eds. *Treatise on Geochemistry*. Oxford: Elsevier-Pergamon, 2003. 391–432
- 19 Nürnberg D, Bijma J, Hemleben C, et al. Assessing the reliability of magnesium in foraminiferal calcite as a proxy for water mass temperatures. *Geochim Cosmochim Acta*, 1996, 60: 803–814
- 20 Elderfield H, Ganssen G. Past temperature and $\delta^{18}\text{O}$ of surface ocean waters inferred from foraminiferal Mg/Ca ratios. *Nature*, 2000, 405: 442–445
- 21 Dekens P S, Lea D W, Pak D K, et al. Core top calibration of Mg/Ca in tropical foraminifera: Refining paleotemperature estimation. *Geochim Geophys Geosyst*, 2002, 3, doi: 10.1029/2001GC000200
- 22 Rosenthal Y, Lohmann G P. Accurate estimation of sea surface temperatures using dissolution-corrected calibrations for Mg/Ca paleothermometry. *Paleoceanography*, 2002, 17: 1044, doi: 10.1029/2001PA000749
- 23 Barker S, Cacho I, Benway H, et al. Planktonic foraminiferal Mg/Ca as a proxy for past oceanic temperatures: a methodological overview and data compilation for the Last Glacial Maximum. *Quat Sci Rev*, 2005, 24: 821–834
- 24 Huang K F, You C F, Lin H L, et al. *In situ* calibration of Mg/Ca ratio in planktonic foraminiferal shell using time series sediment trap: A case study of intense dissolution artifact in the South China Sea. *Geochim Geophys Geosyst*, 2008, 9: Q04016, doi: 10.1029/2007GC001660
- 25 Lea D W, Pak D K, Spero H J. Climate impact of late quaternary equatorial Pacific Sea Surface Temperature variations. *Science*, 2000, 289: 1719–1724
- 26 Lea D W, Pak D K, Belanger C L, et al. Paleoclimate history of Galápagos surface waters over the last 135000 yr. *Quat Sci Rev*, 2006, 25: 1152–1167
- 27 Rashid H, Flower B P, Poore R Z, et al. A ~25 ka Indian Ocean monsoon variability record from the Andaman Sea. *Quat Sci Rev*, 2007, 26: 2586–2597
- 28 Yang W Y, Huang B Q, Xiao J, et al. Environmental changes of surface sea recorded in planktonic foraminifera during MIS 3 in the Western South China Sea (in Chinese). *Quat Sci*, 2008, 8: 437–446
- 29 Hughen K A, Baillie M G L, Bard E, et al. Marine04 Marine radiocarbon age calibration, 0–26 cal kyr BP. *Radiocarbon*, 2004, 46: 1059–1086
- 30 Fairbanks R G, Mortlock R A, Chiu T C, et al. Radiocarbon calibration curve spanning 0 to 50,000 years BP based on paired $^{230}\text{Th}/^{234}\text{U}/^{238}\text{U}$ and ^{14}C dates on pristine corals. *Quat Sci Rev*, 2005, 24: 1781–1796

- 31 Butzin M, Prange M, Lohmann G. Radiocarbon simulations for the glacial ocean: the effects of wind stress, Southern Ocean sea ice and Heinrich events. *Earth Planet Sci Lett*, 2005, 235: 45–61
- 32 Mulitza S, Bolotovskoy D, Donner B, et al. Temperature: $\delta^{18}\text{O}$ relationships of planktonic foraminifera collected from surface waters. *Palaeogeogr Palaeoclimatol Palaeoecol*, 2003, 202: 143–152
- 33 Arz H W, Lamy F, Canopolski A, et al. Dominant Northern Hemisphere climate control over millennial-scale glacial sea-level variability. *Quat Sci Rev*, 2007, 26: 312–321
- 34 Waelbroeck C, Labeyrie L, Michel E, et al. Sea-level and deep water temperature changes derived from benthic foraminifera isotopic records. *Quat Sci Rev*, 2002, 21: 295–305
- 35 North Greenland Ice Core Project members. High-resolution record of Northern Hemisphere climate extending into the last interglacial period. *Nature*, 2004, 431: 147–151
- 36 Jian Z M, Huang B Q, Kuhnt W, et al. Late Quaternary Upwelling intensity and East Asian Monsoon forcing in the South China Sea. *Quat Res*, 2001, 55: 363–370
- 37 Huang B Q, Jian Z M, Cheng X R, et al. Foraminiferal responses to upwelling variations in the South China Sea over the last 220000 years. *Mar Micropaleontol*, 2003, 47: 1–15
- 38 Huang B Q, Jian Z M. Late Quaternary coastal upwelling and variations of the East Asian summer monsoon off the Vietnam coast (in Chinese). *Quat Sci*, 1999, 6: 518–525
- 39 Bühring C, Sarnthein M, Erlenkeuser H. Toward a high-resolution stable isotope stratigraphy of the last 1.1 my: Site 1144, South China Sea. In: Prell W L, Wang P X, Blum P, et al., eds. *Proc ODP, Sci Results*, 2004, 184: 1–29
- 40 Dannenmann S, Linsley B K, Oppo D W, et al. East Asian monsoon forcing of suborbital variability in the Sulu Sea during Marine Isotope Stage 3: Link to Northern Hemisphere climate. *Geochem Geophys Geosyst*, 2003, 4: 1001, doi: 10.1029/2002GC000390
- 41 Stott L, Poulsen C, Lund S, et al. Super ENSO and global climate oscillations at millennial time scales. *Science*, 2002, 297: 222–226
- 42 Haug G H, Hughen K A, Sigman D M, et al. Southward Migration of the Intertropical Convergence Zone through the Holocene. *Science*, 2001, 293: 1304–1308
- 43 Yancheva G, Nowaczyk N R, Mingram J, et al. Influence of the Intertropical convergence zone on the East Asian monsoon. *Nature*, 2007, 445: 74–77
- 44 Broecker W S. Does the Trigger for Abrupt Climate Change Reside in the Ocean or in the Atmosphere? *Science*, 2003, 300: 1519–1522
- 45 Schiller A, Mikolajewicz U, Voss R. The stability of the North Atlantic thermohaline circulation in a coupled ocean-atmosphere general circulation model. *Clim Dyn*, 1997, 13: 325–347
- 46 Koutavas A, Lynch Stieglitz J, Marchitto T M, et al. El Niño like pattern in ice age tropical Pacific sea surface temperature. *Science*, 2002, 297: 226–230